HHS Public Access

Author manuscript

*Dev Cell*. Author manuscript; available in PMC 2017 October 24.

Published in final edited form as:

*Dev Cell*. 2016 October 24; 39(2): 254–266. doi:10.1016/j.devcel.2016.09.017.

# Vamana Couples Fat Signaling to the Hippo Pathway

**Jyoti R. Misra** and **Kenneth D. Irvine**

Howard Hughes Medical Institute, Waksman Institute, and Department of Molecular Biology and Biochemistry, Rutgers University, Piscataway NJ 08854 USA

## SUMMARY

The protocadherins Dachsous and Fat initiate a signaling pathway that controls growth and planar cell polarity by regulating the membrane localization of the atypical myosin Dachs. How Dachs is regulated by Fat signaling has remained unclear. Here we identify the *vamana* gene as playing a crucial role in regulating membrane localization of Dachs, and in linking Fat and Dachsous to Dachs regulation. Vamana, an SH3 domain-containing protein, physically associates with and co-localizes with Dachs, and promotes its membrane localization. Vamana also associates with the Dachsous intracellular domain and with a region of the Fat intracellular domain that is essential for controlling Hippo signaling and levels of Dachs. Epistasis experiments, structure-function analysis, and physical interaction experiments argue that Fat negatively regulates Dachs in a Vamana-dependent process. Our findings establish Vamana as a crucial component of the Dachsous-Fat pathway that transmits Fat signaling by regulating Dachs.

## Graphical abstract

Fat signaling regulates growth and Planar Cell Polarity by regulating the localization of the atypical myosin, Dachs. Misra & Irvine describe the essential role of the adapter protein Vamana in transmitting Fat signaling by physically coupling Dachsous and Fat to Dachs.

Correspondence/Lead Contact: irvine@waksman.rutgers.edu.



**AUTHOR CONTRIBUTIONS**

J.M. designed and performed experiments and wrote the manuscript, K.I. designed experiments and wrote the manuscript.

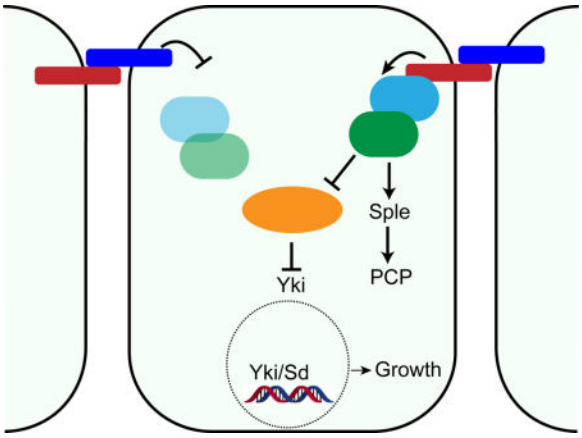


## INTRODUCTION

Coordinated Growth and morphogenesis is critical to development of tissues of specific size and shape. Dachsous (Ds)-Fat signaling (henceforth, Fat signaling) controls both growth, through regulation of Hippo signaling (Irvine and Harvey, 2015; Staley and Irvine, 2012), and morphogenesis, through regulation of planar cell polarity (PCP) (Matis and Axelrod, 2013; Sharma and McNeill, 2013; Thomas and Strutt, 2012). Fat signaling regulates Hippo signaling and PCP by controlling the membrane localization of the atypical myosin protein Dachs (Cho et al., 2006; Mao et al., 2006). Many studies have provided important insights both into how Dachs influences Hippo signaling, and how it influences PCP (Ambegaonkar and Irvine, 2015; Ayukawa et al., 2014; Cho et al., 2006; Mao et al., 2006; Rauskolb et al., 2011; Vrabioiu and Struhl, 2015). In contrast, the mechanism by which Fat signaling actually controls Dachs has remained less well understood.

Fat and Ds are atypical cadherins with novel intracellular domains (ICD), which localize to the plasma membrane just apical to the adherens junctions. Fat and Ds bind to each other in a heterophilic manner, and this interaction is modulated by the Golgi-resident kinase, Four-jointed (Fj), which phosphorylates their extracellular domains (Brittle et al., 2010; Ishikawa et al., 2008; Matakatsu and Blair, 2004; Simon et al., 2010). This heterophilic binding, together with the graded expression of Ds and Fj, contribute to a polarization of Ds and Fat localization within cells (Ambegaonkar et al., 2012; Bosveld et al., 2012; Brittle et al., 2012; Hale et al., 2015). Three different ways by which Fat signaling influences Hippo signaling have been described: Fat signaling influences the membrane localization of Expanded (Ex) (Bennett and Harvey, 2006; Feng and Irvine, 2007; Silva et al., 2006; Willecke et al., 2008), the levels of Wts protein (Cho et al., 2006; Rauskolb et al., 2011), and the interaction of Wts with its cofactor Mats (Vrabioiu and Struhl, 2015). Each of these effects on Hippo signaling depends upon Dachs. Fat signaling affects PCP in at least two ways: through an influence on junctional tension (Bosveld et al., 2012), and by regulating the Spiny-legs isoform of the Prickle locus (Ambegaonkar and Irvine, 2015; Ayukawa et al., 2014; Merkel et al., 2014; Olofsson et al., 2014). Both of these effects also involve Dachs (Fig. 1A).

Dachs was identified as a key downstream effector of Fat signaling because mutations in *dachs* completely suppress the overgrowth induced by *fat* mutations, and partially suppress the PCP defects induced by *fat* mutations (Cho and Irvine, 2004; Mao et al., 2006). Dachs localizes to the cell membrane just apical to the adherens junction in a polarized manner; in the developing wing Dachs is localized to the distal sides of the cell, in response to the proximal-distal gradients of Ds and Fj expression (Ambegaonkar et al., 2012; Brittle et al., 2012; Mao et al., 2006; Rogulja et al., 2008). Dachs membrane localization requires a palmitoyltransferase encoded by *approximated* (*app*), but how App influences Dachs localization is unknown (Matakatsu and Blair, 2008). In *fat* or *ds* mutants increased levels of Dachs are observed at the apical membrane and Dachs is no longer polarized (Ambegaonkar et al., 2012; Brittle et al., 2012; Mao et al., 2006). Forcing Dachs membrane localization by fusing it to Zyxin phenocopies *fat* mutants (Pan et al., 2013). Conversely, overexpression of full length Fat or even just the Fat intracellular domain (ICD) displaces Dachs from the membrane into the cytoplasm (Mao et al., 2006; Rodrigues-Campos and Thompson, 2014). These and other observations have indicated that Fat regulates growth by modulating the levels of Dachs at apical membranes, and regulates Dachs-dependent PCP by directing Dachs asymmetry.

To understand how Fat functions, several studies have examined the roles of different regions of the Fat-ICD (Bossuyt et al., 2014; Matakatsu and Blair, 2012; Pan et al., 2013; Zhao et al., 2013) (Fig. S1A). These studies identified two regions that mediate its growth suppressive function. One, the D region, around amino acids 4975 to 4993, makes a modest contribution to Hippo pathway regulation, as when this region is deleted flies are viable but their wings are approximately 30% larger than normal (Pan et al., 2013), and also rounder than normal. The D region is required for interaction with the ubiquitin ligase, Fbxl7, which reduces Dachs membrane levels, and mutation of which results in phenotypes similar to deletion of the D region (Bosch et al., 2014; Rodrigues-Campos and Thompson, 2014). A second region, which has been referred to as HM (Bossuyt et al., 2014), Hpo (Matakatsu and Blair, 2012), or H2 (Zhao et al., 2013), is defined by observations that deletions within this region block the ability of Fat to activate Hippo signaling (Fig. S1). Two alleles of *fat*, $fat^{61}$ and $fat^{sum}$, have also been identified that harbor mutations within this region, and are associated with tissue overgrowth comparable to that caused by *fat* null mutations (Bosch et al., 2014; Bossuyt et al., 2014). However, the mechanism by which this region, which for simplicity we will refer to as the H region, regulates the Hippo pathway, and whether it affects Dachs, are unknown.

Here we report the isolation and characterization of the SH3-domain containing protein encoded by *vamana (vam).* Loss of *vam* function decreases growth, whereas overexpression of *vam* promotes growth. These effects are mediated through regulation of the Hippo pathway, and we show that *vam* functions genetically downstream of *fat*, as *vam* mutations can suppress both growth and PCP phenotypes of *fat*. Vam localizes to the apical region of epithelial cells in a polarized manner, co-localizing with Dachs, and is required for normal membrane localization of Dachs. Vam physically associates with the carboxy-terminal domain of Dachs and the ICDs of Ds and Fat, and is regulated by the H region of the Fat ICD. Our observations identify Vam as a key mediator of signaling from Fat to Dachs.

# RESULTS

## *vamana* Mutant Phenotypes Resemble *dachs* Mutant Phenotypes

We identified *vam* based on the short crossvein spacing of homozygous adults in flies carrying pUAST-YFP-Rab26-Q250L (Zhang et al., 2007), henceforth referred to as $vam^{04}$. This transgene is inserted in the first coding exon of the *vam* (*CG10933*) locus, immediately after the first five codons (Fig.1B). The homozygous adults identified in this stock, as well hemizygous animals generated by crossing to a chromosomal deficiency that deletes *vam*, display a reduction in wing size and a reduced distance between the anterior and posterior crossveins (Fig. 1D,E,I,J). To confirm that loss of *vam* is responsible for these phenotypes, we created a *vam* null mutant ($vam^{C}$) by replacing the entire *vam* coding region with Ds-Red, through CRISPR-Cas9-assisted cassette exchange (Fig. 1B). Homozygous or hemizygous $vam^{C}$ mutants also display reduced wing area and crossvein spacing (Fig. 1F,G,I,J), and eclose at approximately 2/3 of the expected rate (28/42 expected). Depletion of *vam* by expressing a UAS-RNAi line in the wing under control of *nub-Gal4* causes similar wing phenotypes (Fig. 2).

Reduced crossvein spacing is a characteristic phenotype of mutations in components of the Fat pathway (Bryant et al., 1988; Clark et al., 1995; Mahoney et al., 1991; Mao et al., 2006; 2009; Matakatsu and Blair, 2008; Villano and Katz, 1995), suggesting that *vam* could participate in Fat signaling. The Fat pathway also regulates the growth and shape of the legs. In *vam* mutants, the length of the tarsal region is reduced, and some of the mutant legs are composed of only four tarsal segments instead of five (Fig. 1K–O). A similar reduction in tarsal length is observed in flies depleted of *vam* by RNAi (Fig. S1B–D). The influence of *vam* mutants on wings and legs is similar to that of hypomorphic alleles of *dachs* (Mao et al., 2006).

As the Fat pathway also regulates PCP, we examined *vam* mutant wings for effects on hair polarity. Deviations in the normal distal orientation of wing hairs were observed in the proximal anterior wing in the *vam* mutants, (Fig. S1E–G), where *dachs* mutants can also exhibit disturbed hair polarity (Matakatsu and Blair, 2008). Furthermore, a mild hair orientation defect similar to that seen in *dachs* mutants could be observed in the posterior dorsal abdomen (Fig. S1I–K).

## *vam* is Epistatic to *fat*

To confirm that *vam* affects Fat signaling, and to position the genetic requirement for *vam*, we performed epistasis tests. Strong *fat* mutant alleles are lethal, but when the amorphic *fat* allele $fat^{G\text{-}rv}$ was combined with $vam^{C}$, adult flies could be recovered, at about 1/3 of the expected rate (56/152 expected), and their wings were smaller than wild-type controls (Fig. 2A–C). *fat* mutants also have strong PCP phenotypes, including a mis-orientation of hairs visible in the anterior abdomen of pharate adults; this PCP phenotype was also suppressed by $vam^{c}$ (Fig. S2G–I). Thus *vam* is epistatic to *fat* for viability, wing growth, and PCP.

To further characterize the genetic relationship between *fat* and *vam* we used UAS-RNAi lines. RNAi of *fat* in the wing under *nub-Gal4* control induces wing overgrowth and disturbs wing hair polarity (Fig. 2E,L, Fig. S2C), while depletion of *vam* results in smaller wings

(Fig. 2H,L), similar to those in *vam*$^{c}$ mutants. Simultaneous depletion of both *fat* and *vam* results in phenotypes similar to vam depletion alone: small wings with mostly normal wing hair PCP (Fig. 2 I,L, S2D). Loss of *fat* increases growth by reducing Wts levels and activation, which leads to increased activity of the Hippo pathway transcription factor Yorkie (Yki) (Irvine and Harvey, 2015; Staley and Irvine, 2012). Hence depletion of *fat* in the posterior compartment of wing imaginal discs by expressing RNAi lines under *en-Gal4* control increases expression of the Yki reporter *ex-lacZ* (Fig. 2M,P), whereas depletion of *vam* decreases *ex-lacZ* (Fig. 2M,O). Simultaneous depletion of *fat* and *vam* reduces ex-lacZ similarly to *vam* RNAi (Fig. 2M,Q). Depletion of *ds* results in enlarged wings similar to those observed upon *fat* depletion, and this overgrowth phenotype was also suppressed by depletion of *vam* (Fig 2F,J,L). Conversely, the wing overgrowth phenotype associated with depletion of *ex*, which regulates Yki activity through distinct mechanisms, was not suppressed by *vam* RNAi (Fig. 2G,K,L). In all respects, these results parallel earlier studies examining the relationship of *dachs* to *fat*, *ds*, and *ex*: *dachs* suppresses overgrowth and PCP phenotypes of *ds* and *fat*, but does not suppress the overgrowth phenotype of *ex* (Ambegaonkar and Irvine, 2015; Brittle et al., 2012; Cho et al., 2006; Mao et al., 2006). The epistasis of *vam* to *fat* indicates that *vam* acts downstream of or in parallel to *fat*, while the observation that *vam* suppresses both Hippo and PCP phenotypes of *fat* suggests that Vam acts upstream of the branching of Fat signaling into distinct Hippo and PCP pathways, which occurs downstream of Dachs. Altogether, the observed genetic interactions argue that Vam acts as a component of the Fat signaling pathway, acting at or downstream of Fat, and at or upstream of Dachs.

### *vam* Encodes a SH3-domain Containing Protein with Polarized Membrane Localization

*vam* encodes a 355 amino acid protein predicted to contain 3 Src homology-3 (SH3) domains (Figure S2M). It is evolutionarily conserved among the insects, but does not have close homologs in vertebrates. However, *ab initio* structure prediction by i-TASSER (Yang et al., 2015) suggests that it is structurally similar to the adapter protein CRKII (Fig. S2K,L). Further, its domain organization resembles several SH3 domain-containing proteins, such as, Growth factor receptor-bound protein 2 (Grb2), Sorbin and SH3 domain-containing protein-2 (SORBS2), and Non-catalytic region of tyrosine kinase adaptor protein (NCK). These proteins all function as adapters that assemble protein complexes, and play roles in signaling pathways (Pawson and Scott, 1997).

In order to examine the subcellular localization of Vam, we created transgenic flies carrying a GFP-tagged genomic construct for *vam* (*vam:GFP*), where GFP is fused to the Vam C-terminus. This transgene is fully functional as it can rescue all phenotypes observed in *vam*$^{c}$ mutants, including wing size, crossvein spacing, hair polarity, and tarsal length (Figs 1, S1). Vam:GFP preferentially localizes to the cell membrane with a distribution that is slightly apical to E-cadherin (Fig. 3A). This region, which has been referred to as the sub-apical membrane, or marginal zone, is where Fat and Ds localize, and Vam:GFP localizes along the same apical-basal plane as Fat, Ds, and Dachs (Fig S3). Vam:GFP is not uniformly distributed around the cell circumference, but instead exhibits a punctate distribution (Fig. 3A–C). These Vam puncta overlap extensively with Dachs and Ds puncta (Figs 3B,C, S3). A key feature of Dachs localization in wing discs is that it is preferentially enriched on the

distal sides of cell membranes (Mao et al., 2006). To address whether Vam localization is polarized, we created a Flp-out cassette expressing Vam:GFP under the control of the *Actin-5C* promoter, with an intervening transcriptional stop cassette flanked by FRT sites. Expression of Vam:GFP in clones using this construct through heat shock-induced expression of Flipase revealed that aside from a region near the D–V compartment boundary, where Dachs polarity is also less evident (Merkel et al., 2014), Vam:GFP preferentially localizes to the distal sides of cells (Fig 3D,E). This places Vam on the same sides of cells as Dachs and Ds, and opposite to Fat (Ambegaonkar et al., 2012; Brittle et al., 2012; Mao et al., 2006). The Dachs and Ds-like localization of Vam further supports the conclusion that Vam participates in Fat signaling. This distal and punctate localization of Vam, is however, only observed when it is expressed at endogenous or low levels. When Vam:GFP or Vam:RFP are over-expressed using the UAS-Gal4 system, they appear uniformly distributed along the sub-apical membrane (Fig. S3D).

## Vam Localization is Regulated by Fat Signaling

The observation that Vam co-localizes with Dachs suggests that like Dachs, Vam localization is regulated by Fat signaling. Indeed, depletion of *fat* increased levels of Vam at apical cell junctions without increasing total levels of Vam, and this increased accumulation of Vam on membranes was not polarized (Figs 3F,4A, S4K). Similarly, depletion of *ds* also leads to increased levels at Vam, and loss of Vam polarization, at apical junctions (Fig. 4D). These effects of Fat and Ds on Vam are similar to their effects on Dachs (Ambegaonkar et al., 2012; Mao et al., 2006). Ectopic boundaries of Ds expression can alter the direction of Dachs polarization, as Ds, Fat, and Dachs all become repolarized parallel to the new boundary (Ambegaonkar et al., 2012; Brittle et al., 2012). Similarly, we observed that the direction of Vam polarization could be altered by Ds boundaries created by expression of *UAS-ds* or *UAS-RNAi-ds* under *hh-Gal4* control (Fig. 4B,C).

## Vam and Dachs Promote each other's Membrane Localization

The resemblance of *vam* mutant phenotypes to *dachs* mutant phenotypes, ability of *vam* mutants to suppress *fat* mutant phenotypes, and similar localization of Vam and Dachs in wild-type and mutant backgrounds raised the possibility that *vam* might control Dachs localization or activity. To test this, we examined the effect of loss of *vam* on Dachs localization. In cells lacking *vam*, Dachs levels at apical cell junctions were greatly reduced, while total levels of Dachs were not significantly decreased, and instead Dachs was mostly found in the cytoplasm, often in punctate, presumably vesicular, structures that do not overlap Fat or Ds (Figs 5A, S4A,B, L). Conversely, depletion of *vam* did not significantly affect the localization or levels of Fat or Ds (Fig. S4A,B). Thus, Vam is required for membrane localization of Dachs. Moreover, overexpression of Vam:RFP induced an increase in Dachs:GFP levels at apical junctions (Fig 5B), without significantly increasing total Dachs:GFP levels (Fig S4C), indicating that increasing Vam levels can promote Dachs membrane localization. Consistent with the influence of membrane-localized Dachs on Hippo signaling, overexpression of Vam also increased wing growth and the expression of Yki target genes (Fig. S4F,H–J).

To further investigate the relationship between Vam and Dachs, we asked whether Dachs influences Vam. Depletion of Dachs led to complete loss of Vam membrane localization (Fig. 5C), with Vam still detected in the cytoplasm (Fig. 5C), and total levels of Vam only modestly decreased (Fig S4K). Overexpression of V5-tagged Dachs (*Dachs:V5*) causes upregulation of junctional Vam:GFP (Fig. 5D). Thus, Dachs and Vam are reciprocally required for each other's membrane localization, and increasing the expression of either protein is sufficient to increase membrane levels of the other. This mutual stabilizing effect of Vam and Dachs is also reflected in tissue growth. Overexpression of either Dachs alone or Vam alone modestly promotes wing growth, whereas simultaneous overexpression of both Dachs and Vam together elicited a stronger growth increase (Fig. S4D–H).

## Physical Interaction Between Vam and Dachs

The similar mutant phenotypes and reciprocal regulation of membrane localization of Vam and Dachs suggested that they might physically interact. Interestingly, a large scale proteomics investigation of Hippo pathway interactions reported that Vam associates with Dachs (Kwon et al., 2013). We verified this by co-immunoprecipitation of tagged versions of Vam and Dachs expressed in S2 cells (Fig. 5E,F). To gain further insight into their association, we mapped the regions in each protein that mediate it by expressing tagged truncated versions of Vam and Dachs in S2 cells and assaying for co-immunoprecipitation. We expressed N-terminal (D–N:V5), Middle (D–M:V5), and C-terminal (D–C:V5) fragments of D and assayed for interaction with full length Vam:RFP. Both, full length Dachs:V5, as well as D–C:V5, but not D–N:V5 or D–M:V5, could be co-precipitated by Vam, indicating that the C-terminal region of Dachs mediates association with Vam (Fig. 5E). Given that SH3 domains primarily function as protein-protein interaction modules, in analyzing how Vam interacts with Dachs we examined whether any of the three SH3 domains are required. This revealed that while deleting the first (SH3-1) or third (SH3-3) SH3 domains did not prevent co-precipitation of Dachs by Vam, deleting the second (SH3-2) SH3 domain severely compromised their interaction (Fig.5F). Thus, the second SH3 domain of Vam is preferentially required for association with Dachs.

## Influence of Vam SH3 Domains on Vam and Dachs Localization

To investigate functional requirements for the different SH3 domains of Vam, we created transgenic animals carrying truncated versions of Vam under UAS control, and expressed them in wing discs using *nub-Gal4*. Deletion of any individual SH3 domain did not prevent localization of Vam to apical cell junctions (Fig. 6A,B, S5A–C). A UAS construct expressing the N-terminal region alone, and hence missing all three SH3 domains localizes to the membranes, but in a broader distribution than full-length Vam, as it is also found along basolateral membranes (Fig. S5C). Some peripheral membrane proteins localize to the membrane through palmitoylation. As Vam has an N-terminal cysteine that is predicted to have a high probability of being palmitoylated, and the mutant phenotype of *app* (Matakatsu and Blair, 2008), which encodes a palmitoyltransferase, resembles that of *vam*, we considered the possibility that Vam might be palmitoylated. Depletion of *app* by RNAi prevents Vam membrane localization (Fig. S5F), but this could be an indirect consequence of the influence of App on Dachs membrane localization. We assayed directly for palmitoylation of Vam using an acyl-biotin exchange assay, but no evidence of

palmitoylation was detected (Fig. S5G). Additionally, when we mutated the predicted palmitoylation site near the N terminus of Vam (Cysteine 5 to Serine, C5S) it did not prevent Vam membrane localization (Fig. S5I), although it did result in accumulation of Vam in the cytoplasm (Fig. S5I′).

To assess contributions of the SH3 domains to Dachs regulation, we performed rescue experiments using SH3 domain deletion constructs. Endogenous *vam* was depleted using an RNAi construct that targets 18 bases in the *vam* coding sequence. We then created RNAi-resistant *vam* transgenes in which this sequence was altered, without changing the amino acid sequence, by using alternate codons. In this assay, full length Vam, Vam-ΔSH3-1 and VamΔSH3-3 efficiently rescued the Vam RNAi phenotype, as evidenced by reduced cytoplasmic and increased membrane accumulation of Dachs (Fig.6C,D, S5D,E). Conversely, Vam-ΔSH3-2 was much less effective at rescuing Dachs localization (Fig. 6E). Thus, the SH3-1 and SH3-3 domains of Vam are at least individually dispensable for Dachs localization, where as SH3-2 is required for Vam to correctly localize Dachs.

## Physical Interaction of Vam with Fat and Ds

Dachs co-localizes in puncta with Ds (Ambegaonkar et al., 2012; Bosveld et al., 2012; Brittle et al., 2012), and it has been reported that tagged isoforms of Dachs and Ds could be co-precipitated from lysates of cultured cells (Bosveld et al., 2012). Since Vam co-localizes in puncta with Dachs and Ds, we examined if Vam also associates with the Ds ICD. Indeed, when tagged isoforms of Vam and the Ds ICD were expressed in S2 cells, they could be co-immunoprecipitated (Fig.6F). This interaction was mediated principally by the first and third SH3 domains of Vam, rather than the second, because these SH3 domains individually could co-precipitate the Ds-ICD much more effectively than the second SH3 domain (Fig. 6F). Intriguingly, we obtained similar results investigating the potential for interaction between Vam and the Fat ICD: co-immunoprecipitation assays revealed that tagged full length Vam, as well as Vam lacking any one of the three SH3 domains, physically interacts with the Fat-ICD (Fig. 6G). Analysis of individual SH3 domains revealed that both the SH3-1 and SH3-3 domains interact strongly with Fat-ICD, whereas SH3-2 interacted much more weakly (Fig. 6G) Interaction of full length Vam with Fat or Ds also appears to be slightly weaker than that of the isolated SH3-1 or SH3-3 domains, which could result from reduced accessibility of these domains within the intact protein.

## Regulation of Vam by the H Region of Fat

To further characterize the interaction between the Fat ICD and Vam, we assayed for co-precipitation of Vam using truncated versions of Fat. Fat constructs C-terminally truncated at Fat amino acid 5023 (Ft-STI-3) or 4885 (Ft-STI-2) were robustly co-precipitated by Vam:RFP, whereas a truncation to amino acid 4725 (FT-STI-1) was precipitated at background levels (these Fat constructs appear as multiple bands because of endogenous endoproteolytic cleavage of Fat near the membrane, (Feng and Irvine, 2009; Sopko et al., 2009)) (Fig. 7A). These observations implicate the region from 4726 to 4885 as required for association of Fat with Vam. Intriguingly, this overlaps with the H region (Fig. 7A), defined by deletions that impair regulation of Hippo signaling by Fat (Bossuyt et al., 2014; Matakatsu and Blair, 2012; Zhao et al., 2013) (Fig. S1A). Further mapping revealed that

when smaller fragments of the Fat ICD were examined, fragments corresponding to the H2 deletion (Zhao et al., 2013), and more C-terminal regions, could each co-precipitate with Vam, albeit more weakly than the full length ICD (Fig. S6).

Over-expression of either full length Fat, or Fat constructs lacking the extracellular domain (ΔECD) reduce Vam levels at apical junctions (Figs 7F,S6E). These effects of Fat on Vam are similar to its effects on Dachs (Mao et al., 2006; Rodrigues-Campos and Thompson, 2014) (Figs 7B, S6A). To determine whether the H region of the Fat ICD acts by regulating Vam and Dachs membrane localization, we expressed a series of constructs including or lacking this region (Fig. 7J). A C-terminal truncation that does not affect the H region (Fat-ΔECD-Δ6C) efficiently removed both Dachs and Vam from apical cell junctions, whereas constructs with deletions that remove all or part of the H region (Fat-ΔECD-Δ5C, Fat-ΔECD-Δ5-6, Fat-ΔECD-Δ3-5, Fat-ΔH2) fail to remove Dachs or Vam from cell junctions (Figs 7, S6, S7). In fact, expression of Fat-ΔECD-Δ5-6, Fat-ΔECD-Δ3-5, or Fat-ΔH2 interfere with the ability of endogenous Fat to regulate Vam and Dachs, because they increase junctional levels of Vam and Dachs, suggestive of a dominant-negative effect. Finally, expression of a construct comprising the central part of the H region fused to the Fat transmembrane domain (UAS-Fat$^{3Only}$) (Bossuyt et al., 2014) could modestly reduce levels of Dachs and Vam at apical junctions (Fig. S6D,H). Together with studies linking the H region to regulation of Hippo signaling by Fat, these observations implicate regulation of Dachs and Vam levels as the crucial mechanism by which Hippo signaling is controlled by the Fat H region.

## DISCUSSION

Fat and Ds initiate a signaling pathway that controls growth and PCP through regulation of Dachs (Matis and Axelrod, 2013; Staley and Irvine, 2012), but how this occurs has remained poorly understood. We have described here the identification of the *vam* gene, which is genetically required for both overgrowth and PCP phenotypes of *fat*, and which controls Dachs protein localization. Vam localizes to the sub-apical membrane, where it co-localizes with Dachs and Ds, and Vam localization is regulated, together with Dachs, by Ds and Fat. Vam associates with Fat, Ds, and Dachs, enabling it to serve as a physical link between them. Together these observations identify Vam as a crucial component of the Fat signaling pathway that links Fat to regulation of Dachs.

Our studies identified the C-terminal region of Dachs as sufficient to mediate its interaction with Vam. Interestingly, the original *dachs* allele, described almost a century ago by Bridges and Morgan (Bridges and Morgan, 1919), is a hypomorphic allele associated with insertion of a blood transposon just upstream of the C-terminal region (Mao et al., 2006). Hence this allele likely encodes for a truncated protein that lacks the Vam-interaction domain. Consistent with this inference, the *vam* null phenotype appears similar to the *dachs*$^{1}$ phenotype (Mao et al., 2006). Thus, a requirement for interaction with Vam can explain the basis for the original identification of *dachs*.

Vam is evolutionarily conserved among insects but with no close homologs in vertebrates. This is consistent with the fact that Dachs is also only found in insects, and the sequence of

the H region is not conserved in vertebrate Fat genes (Bossuyt et al., 2014; Mao et al., 2006). Nonetheless, Vam is structurally related to a broad family of SH2 and SH3 domain-containing proteins exemplified by CRK, Grb2, Myd88, and NCK. These proteins are referred to as Signal Transducing Adapter Proteins and facilitate formation of protein complexes that play key roles in signal transduction (Flynn, 2001; Pawson and Scott, 1997). Vam is composed of just three SH3 domains; this domain organization is most similar to that of the NCK family of adapters, which contain three SH3 domains along with one SH2 domain (Wunderlich et al., 1999). Our finding that Vam uses both SH3-1 and SH3-3 to interact with Fat and Ds is also reminiscent of NCK family adapters, as they engage effectors using multiple SH3 domains (Wunderlich et al., 1999). The *Drosophila* ortholog of NCK, *dreadlocks* (dock), interacts with cell adhesion molecules encoded by *hibris*, *kirre*, *roughest* and *sticks and stones* (*sns*) to regulate actin polymerization and growth cone migration, and functional redundancy of SH3 domains has been observed for *dock* (Rao and Zipursky, 1998). Multiple SH3 domains are also commonly observed in proteins involved in vesicular trafficking. The observation that in *vam* mutants Dachs accumulates in cytoplasmic puncta that could be vesicular structures suggests that Vam might influence trafficking of Dachs.

Fat and Ds proteins are conserved in vertebrates, where they play important roles in controlling PCP (Mao et al., 2011; 2016; Saburi et al., 2012; 2008; Zakaria et al., 2014), and have also been proposed to influence Hippo signaling (Das et al., 2013). In the absence of a Dachs homologue, however, it has been unclear how downstream signaling is mediated in vertebrate Ds-Fat pathways. The discovery that Vam links Ds and Fat to downstream signaling raises the possibility that a different member of the Signal Transducing Adapter Proteins could mediate downstream Ds-Fat signaling in vertebrates.

The H region of the Fat ICD plays a crucial role in Hippo pathway regulation (Bossuyt et al., 2014; Matakatsu and Blair, 2012; Zhao et al., 2013). Our analysis of Fat ICD truncations revealed that the H region inhibits Vam and Dachs membrane accumulation, the influence of Fat ICD deletions on Hippo signaling correlates with their influence on Vam and Dachs membrane localization, and that the H region of Fat can associate with Vam. Together with observations that Vam associates with and regulates Dachs, these observations lead us to infer that the H region normally functions to promote Hippo signaling through its association with, and regulation of, Vam. Fat also influences growth and Dachs accumulation through a second region of the ICD, the D region (Pan et al., 2013), which interacts with Fbxl7. Because mutation of the D region, or mutations in *Fbxl7* (Bosch et al., 2014; Rodrigues-Campos and Thompson, 2014), have weaker phenotypes than mutations in the H region, the H region appears to play the larger role in Dachs regulation, but we nonetheless expect that both regions normally act in parallel to regulate membrane levels of Dachs, and thus ultimately, Hippo signaling.

The localization of Vam in different genotypes, together with its physical interactions, suggests models for how Vam regulates Dachs localization (Fig. 7K). Since Vam and Dachs are reciprocally required for each other's membrane localization, we infer that a complex between these two proteins is required for their stable localization to apical junctions, where Dachs regulates PCP (via interactions with Sple) and Hippo signaling (via interactions with

Zyxin and Warts). The observations that Fat promotes removal of Vam and Dachs from the sub-apical membrane, associates with Vam, yet doesn't visibly co-localize with Vam at apical junctions, suggests that Fat normally removes Vam-Dachs complexes from the sub-apical membrane. One mechanism by which this might occur is through binding of Fat to Vam, followed by endocytosis of Fat-Vam-Dachs complexes. Alternatively, Fat binding might disrupt Vam-Dachs binding, as these proteins normally do not localize to the membrane in isolation.

We also observed that Vam can interact with the Ds ICD, and that it does so through the same SH3 domains as it uses to interact with the Fat ICD. This suggests that these interactions are likely to be competitive. In this case, interaction of Vam with the Ds ICD could promote Vam and Dachs membrane localization by opposing the influence of Fat on Vam. For example, by competing with Fat for binding to Vam, Ds could prevent Fat from disrupting Vam-Dachs interactions, or promoting endocytosis of a Vam-Dachs complex. Consistent with this suggestion that the Ds ICD stabilizes Vam and Dachs at apical junctions, Vam, Ds, and Dachs normally all co-localize in puncta on the distal side of wing cells. The ability of Vam to associate with the ICDs of both Fat and Ds could thus provide a simple mechanism explaining how the ICD of Ds seems to promote Dachs membrane localization, whereas the ICD of Fat inhibits it.

## EXPERIMEMTAL PROCEDURES

### *Drosophila* Strains

The following alleles were used, $ft^{8}$, $ft^{G\text{-}rv}$, $d^{GC13}$, $d^{210}$, *Df(2R)BSC345*, *en-Gal4*, *nub-Gal4*, *tub-Gal4*, *Ay-Gal4*, *hh-Gal4*, *UAS-dcr2*, *ex-lacZ*, *ban-lacZ*, *D:GFP* (Bosveld et al., 2012), *Act>stop> D:GFP* (Brittle et al., 2012), *UAS-Dachs:V5* (Mao et al., 2006), *UAS-ds* (Matakatsu and Blair, 2004), *UAS-Fat, UAS-Fat-ΔECD, UAS-Fat-ΔECD-Δ6C, UAS-Fat-ΔECD-Δ5-C, UAS-Fat-ΔECD-Δ3-5, UAS-Fat-ΔECD-Δ5-6* (Matakatsu and Blair, 2006), $UAS\text{-}Fat^{3Only}$ (Bossuyt et al., 2014) *UAS-Fat-ΔH2* (Zhao et al., 2013) *UAS-vam-RNAi (BL38263), UAS-fat-RNAi (VDRC 9396), UAS-ds-RNAi (VDRC4313), UAS-d-RNAi (VDRC 12555), UAS-app-RNAi* (Matakatsu and Blair, 2008), $vam^{04}$*/CyO,* $vam^{c}$*/CyO,* $vam^{c}$ *FRT42D/CyO, His2-mRFP FRT42D/CyO UAS-vam-3x-FLAG-GFP, UAS-vam-CS-3x-FLAG-GFP, UAS-vam-3x-FLAG-RFP, UAS-vam-ΔSH3-1-3x-FLAG-RFP, UAS-vam-ΔSH3-2-3x-FLAG-RFP, UAS-vam-ΔSH3-3-3x-FLAG-RFP, UAS-vam-N-3x-FLAG-RFP and Act>Stop>-Vam-3x-FLAG-GFP*.

### Immunohistochemistry

Dissected wing discs were fixed in 4% paraformaldehyde for 8 minutes at room temperature and stained with primary antibodies, rat anti-E-cad (1:400, DSHB DCAD2), rat-anti-Fat (1:4000) (Feng and Irvine, 2009), rat-anti-Ds (1: 5000) (Ma et al., 2003), rat-anti-Dachs (1:200) (Brittle et al., 2012) mouse-anti-Wg (1:400, DSHB), mouse anti-ß-gal (1:400, DSHB JIE7-c); and secondary antibodies, donkey anti-rat-647 (1:100, Jackson, 712-605-150) and donkey anti-rat-Cy3 (3:400, Jackson, 712-165-150). GFP and RFP were detected by autofluorescence. Confocal images were captured using a Leica SP5 laser scanning microscope. All scale bars indicate 12uM, unless otherwise specified.

### Cell culture and Immunoprecipitation

S2 cells were grown in Schneider's media and transfected with plasmids aw-GAL4, pUAST-D-FL:V5 (Mao et al., 2006) pUAST-D-N:V5, pUAST-D-M:V5, pUAST-D-C:V5 (Rauskolb et al., 2011), pUAST-GFP:V5, pUAST-vam-FL-RFP, pUAST-vam-ΔSH3-1-RFP, pUAST-vam-ΔSH3-2-RFP, pUAST-vam-ΔSH3-3-RFP, pUAST-Fat-Fat-ICD:V5, pUAST-Ds-ICD:V5 (Mao et al., 2009) pUAST-Fat-STI, pUAST-Fat-STI-1, pUAST-Fat-STI-2, pUAST-Fat-STI-3 (Feng and Irvine, 2009), using Effectene transfection reagent (Quiagen) following manufacturer's instruction. Cells were lysed in RIPA buffer supplemented with protease inhibitor cocktail (Roche) and phosphatase inhibitor cocktail (Calbiochem). Cell lysates were incubated with RFP-trap beads (Chromotek) for two hours at 4 °C, following which they were washed four times. Pr oteins samples were boiled with Laemlii buffer and subjected to SDS-PAGE using 4–15% gradient gels (Bio Rad). Western transfer was carried out using Trans-Blot Turbo transfer system (Bio Rad) and immunoblotting was performed using the primary antibodies, rabbit-anti-tRFP (1:10000) (Evrogen), mouse anti-v5(1:5000) (Invitrogen), mouse-anti-GAPDH(1:1000) (Bethyl Laboratories), Rabbit-anti-GAPDH (1:1000) (Bethyl laboratories), rabbit-anti-GFP (1:1000) (Invitrogen); and as secondary antibodies goat anti-mouse 680 (Li-Cor, 926–68,020), goat anti-rabbit-680 (Li-Cor, 926–68,021), all at a dilution of 1:10,000. Blots were scanned using an Odyssey Imaging System (Li-Cor). Seven independent biological replicates were performed for co-immunoprecipitation experiments for interaction of Vam:RFP with Ds-ICD and Fat-ICD (Fig. 6 F,G), five biological replicates were performed for co-immunoprecipitation experiments for interaction of Vam:RFP with Dachs (Fig. 5 E,F) and three biological replicates were performed for interaction between Vam:RFP and Fat-STI constructs, and between Vam-RFP and Fat-H2 (Figure 6 I).

### Acyl Biotin Exchange Assay

Acyl Biotin Exchange Assay was carried out as previously described (Brigidi and Bamji, 2013). Briefly, S2 cells were transfected with pUAST-Vam-V5 or pUAST-Vam (C5S)-V5 with or without pUAST-App and cells were lysed in buffer containing 50mM NEM and Vam was immunoprecipitated using anti-V5 agarose (Sigma) and subjected to HAM cleavage with 1M HAM for 1 hour at room temperature, following which it was incubated with 1uM BMCC-biotin for 1 hour at room temperature. After thorough wash, the protein was boiled in Laemmli buffer and subjected to SDS-PAGE followed by Western transfer. Immunoblotting was performed using Rabbit anti-V5 primary antibody and goat anti-rabbit-800 (Licor) secondary antibody. IRDye-680RD-Streptavidin (Licor 925-68079) was used at 1:10000 dilution to detect biotin, and the blots were scanned using an odyssey imaging system.

### Prediction of Vam Structure and Palmitoylation

Structure prediction of Vam was carried out using the *ab initio* prediction program i-TASSER (http://zhanglab.ccmb.med.umich.edu/I-TASSER/) (Yang et al., 2015). The structure with the lowest C score (−2.19) was used for determination of structural similarity by the TM-align, structural alignment program of the i-TASSER suite and the structure with

highest alignment score is shown (Fig S2). Palmitoylation prediction was carried out using the CSS-Palm (Ren et al., 2008) and PalmPred (Kumari et al., 2014) programs.

### Quantification of Vam:GFP polarization

For quantification of Vam:GFP polarity, third instar larvae carrying heat shock inducible flippase (*hs-FLP*) and attb-pAct-FRT-Stop-FRT-vam-3x-FLAG-GFP were subjected to heat shock at 37°C for 5 minutes and dissected after 20–24 hours, following which they were fixed and stained with rat anti-Ecad and mouse anti-Wg antibodies. Most of the clones contained about 2–4 cells. Using the Wg staining as the dorsal-ventral compartment boundary (distal), individual cells in a clone were visually analyzed for preferential enrichment of Vam-GFP at the apical junction using Ecad as a marker. More then 600 cells were scored and the percentage of cells exhibiting, distal, proximal or neutral polarity of Vam:GFP were graphed. The cells in clones that were close to the D–V boundary often failed to exhibit clear distal polarity, as has been reported for Dachs (Merkel et al., 2014; Schwank et al., 2011).

### Quantification of lacZ levels

Quantification of lacZ levels was performed from confocal stacks using a 3D image analysis program (Volocity) as reported earlier (Rauskolb et al., 2014). Briefly, nuclei were identified by Hoechst staining as the ß-gal encoded by ex-lacZ has a nuclear localization signal. Mean intensity per nuclear volume for ß-gal staining was measured from the four quadrants of the wing pouch avoiding the compartment boundaries and the edge of the wing pouch. Posterior to anterior (P/A) ratio was calculated for individual discs and the P/A ratios were normalized to the control.

### Statistical Analyses

Statistical significance was calculated using Graphpad Prism Software. For pairwise comparisons we used t tests and for comparison of ratios, statistical tests were done on log transforms of the ratios.

Additional Methods are in the Supplemental Material

## Supplementary Material

Refer to Web version on PubMed Central for supplementary material.

## Acknowledgments

We thank the Developmental Studies Hybridoma Bank, Bloomington *Drosophila* stock center, D. Strutt, I. Hariharan, M. Simon, G. Halder, Y. Bellaiche and S. Blair for providing *Drosophila* stocks and antibodies. This research was supported by NIH grant R01 GM078620 and the Howard Hughes Medical Institute.

## References

Ambegaonkar AA, Irvine KD. Coordination of planar cell polarity pathways through Spiny legs. Elife. 2015; 4:e09946. [PubMed: 26505959]

Ambegaonkar AA, Pan G, Mani M, Feng Y, Irvine KD. Propagation of Dachsous-Fat planar cell polarity. Curr Biol. 2012; 22:1302–1308. [PubMed: 22727698]

Ayukawa T, Akiyama M, Mummery-Widmer JL, Stoeger T, Sasaki J, Knoblich JA, Senoo H, Sasaki T, Yamazaki M. Dachsous-dependent asymmetric localization of spiny-legs determines planar cell polarity orientation in Drosophila. Cell Rep. 2014; 8:610–621. [PubMed: 24998533]

Bennett FC, Harvey KF. Fat cadherin modulates organ size in Drosophila via the Salvador/Warts/Hippo signaling pathway. Curr Biol. 2006; 16:2101–2110. [PubMed: 17045801]

Bosch JA, Sumabat TM, Hafezi Y, Pellock BJ, Gandhi KD, Hariharan IK. The Drosophila F-box protein Fbxl7 binds to the protocadherin fat and regulates Dachs localization and Hippo signaling. Elife. 2014; 3:e03383. [PubMed: 25107277]

Bossuyt W, Chen CL, Chen Q, Sudol M, McNeill H, Pan D, Kopp A, Halder G. An evolutionary shift in the regulation of the Hippo pathway between mice and flies. Oncogene. 2014; 33:1218–1228. [PubMed: 23563179]

Bosveld F, Bonnet I, Guirao B, Tlili S, Wang Z, Petitalot A, Marchand R, Bardet PL, Marcq P, Graner F, et al. Mechanical control of morphogenesis by Fat/Dachsous/Four-jointed planar cell polarity pathway. Science. 2012; 336:724–727. [PubMed: 22499807]

Bridges CB, Morgan TH. Contributions to the genetics of Drosophila melanogaster. II. The second-chromosome group of mutant characters. Carnegie Inst Washington Publ. 1919; 278:123–304.

Brittle AL, Repiso A, Casal J, Lawrence PA, Strutt D. Four-jointed modulates growth and planar polarity by reducing the affinity of dachsous for fat. Curr Biol. 2010; 20:803–810. [PubMed: 20434337]

Brittle A, Thomas C, Strutt D. Planar polarity specification through asymmetric subcellular localization of Fat and Dachsous. Curr Biol. 2012; 22:907–914. [PubMed: 22503504]

Bryant PJ, Huettner B, Held LI, Ryerse J, Szidonya J. Mutations at the fat locus interfere with cell proliferation control and epithelial morphogenesis in Drosophila. Dev Biol. 1988; 129:541–554. [PubMed: 3417051]

Cho E, Irvine KD. Action of fat, four-jointed, dachsous and dachs in distal-to-proximal wing signaling. Development. 2004; 131:4489–4500. [PubMed: 15342474]

Cho E, Feng Y, Rauskolb C, Maitra S, Fehon R, Irvine KD. Delineation of a Fat tumor suppressor pathway. Nat Genet. 2006; 38:1142–1150. [PubMed: 16980976]

Clark HF, Brentrup D, Schneitz K, Bieber A, Goodman C, Noll M. Dachsous encodes a member of the cadherin superfamily that controls imaginal disc morphogenesis in Drosophila. Genes Dev. 1995; 9:1530–1542. [PubMed: 7601355]

Das A, Tanigawa S, Karner CM, Xin M, Lum L, Chen C, Olson EN, Perantoni AO, Carroll TJ. Stromal-epithelial crosstalk regulates kidney progenitor cell differentiation. Nat Cell Biol. 2013; 15:1035–1044. [PubMed: 23974041]

Feng Y, Irvine KD. Fat and expanded act in parallel to regulate growth through warts. Proceedings of the National Academy of Sciences. 2007; 104:20362–20367.

Feng Y, Irvine KD. Processing and phosphorylation of the Fat receptor. Proceedings of the National Academy of Sciences. 2009; 106:11989–11994.

Flynn DC. Adaptor proteins. Oncogene. 2001; 20:6270–6272. [PubMed: 11607828]

Hale R, Brittle AL, Fisher KH, Monk NAM, Strutt D. Cellular interpretation of the long-range gradient of Four-jointed activity in the Drosophila wing. Elife. 2015; 4:e05789.

Irvine KD, Harvey KF. Control of organ growth by patterning and hippo signaling in Drosophila. Cold Spring Harbor Perspectives in Biology. 2015; 7

Ishikawa HO, Takeuchi H, Haltiwanger RS, Irvine KD. Four-jointed is a Golgi kinase that phosphorylates a subset of cadherin domains. Science. 2008; 321:401–404. [PubMed: 18635802]

Kwon Y, Vinayagam A, Sun X, Dephoure N, Gygi SP, Hong P, Perrimon N. The Hippo signaling pathway interactome. Science. 2013; 342:737–740. [PubMed: 24114784]

Ma D, Yang CH, McNeill H, Simon MA, Axelrod JD. Fidelity in planar cell polarity signalling. Nature. 2003; 421:543–547. [PubMed: 12540853]

Mahoney PA, Weber U, Onofrechuk P, Biessmann H, Bryant PJ, Goodman CS. The fat tumor suppressor gene in Drosophila encodes a novel member of the cadherin gene superfamily. Cell. 1991; 67:853–868. [PubMed: 1959133]

Mao Y, Kucuk B, Irvine KD. Drosophila lowfat, a novel modulator of Fat signaling. Development. 2009; 136:3223–3233. [PubMed: 19710173]

Mao Y, Mulvaney J, Zakaria S, Yu T, Morgan KM, Allen S, Basson MA, Francis-West P, Irvine KD. Characterization of a Dchs1 mutant mouse reveals requirements for Dchs1-Fat4 signaling during mammalian development. Development. 2011; 138:947–957. [PubMed: 21303848]

Mao Y, Rauskolb C, Cho E, Hu WL, Hayter H, Minihan G, Katz FN, Irvine KD. Dachs: an unconventional myosin that functions downstream of Fat to regulate growth, affinity and gene expression in Drosophila. Development. 2006; 133:2539–2551. [PubMed: 16735478]

Mao Y, Kuta A, Crespo-Enriquez I, Whiting D, Martin T, Mulvaney J, Irvine KD, Francis-West P. Dchs1-Fat4 regulation of polarized cell behaviours during skeletal morphogenesis. Nat Commun. 2016; 7:11469. [PubMed: 27145737]

Matakatsu H, Blair SS. Interactions between Fat and Dachsous and the regulation of planar cell polarity in the Drosophila wing. Development. 2004; 131:3785–3794. [PubMed: 15240556]

Matakatsu H, Blair SS. Separating the adhesive and signaling functions of the Fat and Dachsous protocadherins. Development. 2006; 133:2315–2324. [PubMed: 16687445]

Matakatsu H, Blair SS. The DHHC palmitoyltransferase approximated regulates Fat signaling and Dachs localization and activity. Curr Biol. 2008; 18:1390–1395. [PubMed: 18804377]

Matakatsu H, Blair SS. Separating planar cell polarity and Hippo pathway activities of the protocadherins Fat and Dachsous. Development. 2012; 139:1498–1508. [PubMed: 22399682]

Matis M, Axelrod JD. Regulation of PCP by the Fat signaling pathway. Genes Dev. 2013; 27:2207–2220. [PubMed: 24142873]

Merkel M, Sagner A, Gruber FS, Etournay R, Blasse C, Myers E, Eaton S, Jülicher F. The Balance of Prickle/Spiny-Legs Isoforms Controls the Amount of Coupling between Core and Fat PCP Systems. Curr Biol. 2014; 24:2111–2123. [PubMed: 25201685]

Olofsson J, Sharp KA, Matis M, Cho B, Axelrod JD. Prickle/spiny-legs isoforms control the polarity of the apical microtubule network in planar cell polarity. Development. 2014; 141:2866–2874. [PubMed: 25005476]

Pan G, Feng Y, Ambegaonkar AA, Sun G, Huff M, Rauskolb C, Irvine KD. Signal transduction by the Fat cytoplasmic domain. Development. 2013; 140:831–842. [PubMed: 23318637]

Pawson T, Scott JD. Signaling through scaffold, anchoring, and adaptor proteins. Science. 1997; 278:2075–2080. [PubMed: 9405336]

Rao Y, Zipursky SL. Domain requirements for the Dock adapter protein in growth- cone signaling. Proceedings of the National Academy of Sciences of the United States of America. 1998; 95:2077–2082. [PubMed: 9482841]

Rauskolb C, Pan G, Reddy BV, Oh H, Irvine KD. Zyxin links fat signaling to the hippo pathway. PLoS Biol. 2011; 9:e1000624. [PubMed: 21666802]

Rodrigues-Campos M, Thompson BJ. The ubiquitin ligase FbxL7 regulates the Dachsous-Fat-Dachs system in Drosophila. Development. 2014; 141:4098–4103. [PubMed: 25256343]

Rogulja D, Rauskolb C, Irvine KD. Morphogen control of wing growth through the Fat signaling pathway. Dev Cell. 2008; 15:309–321. [PubMed: 18694569]

Saburi S, Hester I, Goodrich L, McNeill H. Functional interactions between Fat family cadherins in tissue morphogenesis and planar polarity. Development. 2012; 139:1806–1820. [PubMed: 22510986]

Saburi S, Hester I, Fischer E, Pontoglio M, Eremina V, Gessler M, Quaggin SE, Harrison R, Mount R, McNeill H. Loss of Fat4 disrupts PCP signaling and oriented cell division and leads to cystic kidney disease. Nat Genet. 2008; 40:1010–1015. [PubMed: 18604206]

Sharma P, McNeill H. Fat and Dachsous cadherins. Prog Mol Biol Transl Sci. 2013; 116:215–235. [PubMed: 23481197]

Silva E, Tsatskis Y, Gardano L, Tapon N, McNeill H. The tumor-suppressor gene fat controls tissue growth upstream of expanded in the hippo signaling pathway. Curr Biol. 2006; 16:2081–2089. [PubMed: 16996266]

Simon MA, Xu A, Ishikawa HO, Irvine KD. Modulation of fat:dachsous binding by the cadherin domain kinase four-jointed. Curr Biol. 2010; 20:811–817. [PubMed: 20434335]

Sopko R, Silva E, Clayton L, Gardano L, Barrios-Rodiles M, Wrana J, Varelas X, Arbouzova NI, Shaw S, Saburi S, et al. Phosphorylation of the tumor suppressor fat is regulated by its ligand Dachsous and the kinase discs overgrown. Curr Biol. 2009; 19:1112–1117. [PubMed: 19540118]

Staley BK, Irvine KD. Hippo signaling in Drosophila: recent advances and insights. Dev Dyn. 2012; 241:3–15. [PubMed: 22174083]

Thomas C, Strutt D. The roles of the cadherins Fat and Dachsous in planar polarity specification in Drosophila. Dev Dyn. 2012; 241:27–39. [PubMed: 21919123]

Villano JL, Katz FN. four-jointed is required for intermediate growth in the proximal-distal axis in Drosophila. Development. 1995; 121:2767–2777. [PubMed: 7555705]

Vrabioiu AM, Struhl G. Fat/Dachsous Signaling Promotes Drosophila Wing Growth by Regulating the Conformational State of the NDR Kinase Warts. Dev Cell. 2015; 35:737–749. [PubMed: 26702832]

Willecke M, Hamaratoglu F, Sansores-Garcia L, Tao C, Halder G. Boundaries of Dachsous Cadherin activity modulate the Hippo signaling pathway to induce cell proliferation. Proceedings of the National Academy of Sciences. 2008; 105:14897–14902.

Wunderlich L, Gohér A, Faragó A, Downward J, Buday L. Requirement of multiple SH3 domains of Nck for ligand binding. Cell Signal. 1999; 11:253–262. [PubMed: 10372803]

Yang J, Yan R, Roy A, Xu D, Poisson J, Zhang Y. The I-TASSER Suite: protein structure and function prediction. Nat Methods. 2015; 12:7–8. [PubMed: 25549265]

Zakaria S, Mao Y, Kuta A, Ferreira de Sousa C, Gaufo GO, McNeill H, Hindges R, Guthrie S, Irvine KD, Francis-West PH. Regulation of neuronal migration by Dchs1-Fat4 planar cell polarity. Curr Biol. 2014; 24:1620–1627. [PubMed: 24998526]

Zhang J, Schulze KL, Hiesinger PR, Suyama K, Wang S, Fish M, Acar M, Hoskins RA, Bellen HJ, Scott MP. Thirty-one flavors of Drosophila rab proteins. Genetics. 2007; 176:1307–1322. [PubMed: 17409086]

Zhao X, Yang CH, Simon MA. The Drosophila Cadherin Fat regulates tissue size and planar cell polarity through different domains. PloS One. 2013; 8:e62998. [PubMed: 23667559]

## Highlights

- *vamana* is a key component of Fat signaling that controls growth and PCP
- *vamana* encodes an SH3 domain-containing adapter protein that regulates Dachs
- Vamana associates with Dachs and with the intracellular domains of Fat and Ds
- The H region of the Fat intracellular domain negatively regulates Vam and Dachs

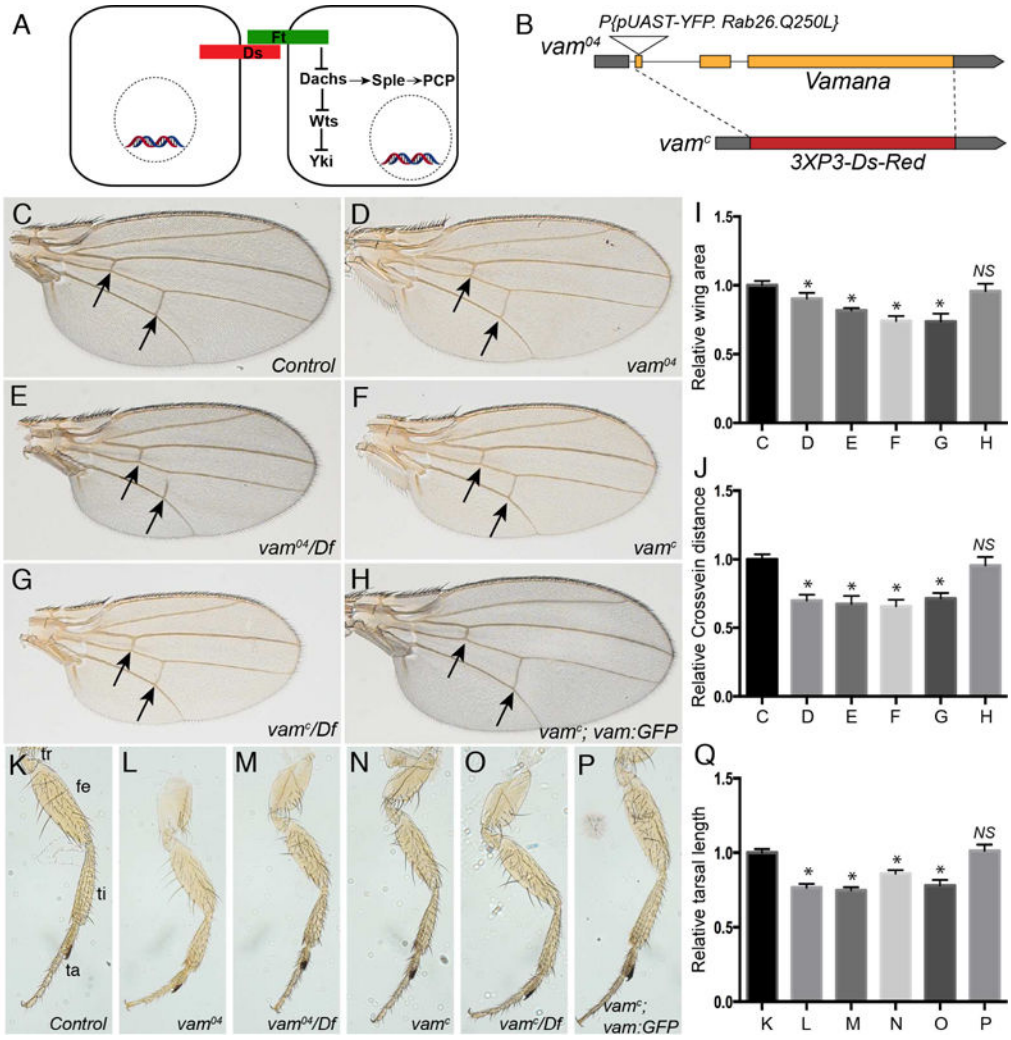


**Figure 1. *vam* Mutant Phenotypes**

(A) Simplified schematic showing the Fat signaling pathway, which regulates PCP and Yki through Dachs. (B) Map of the *Vam* (*CG10933*) transcription unit. The boxes denote the exons and the lines denote introns. The grey indicates untranslated regions and yellow indicates ORF. The triangle denotes the insertion of the P-element in the $vam^{04}$ allele. The lower panel depicts replacement of the *vam* coding sequence by the *3xP3-Ds-Red* cassette (red) in the $vam^{c}$ allele, with the dashed lines marking the boundaries of the replaced sequence. (C–H) Adult male wings from wild-type control (C), homozygous $vam^{04}$ (D), hemizygous $vam^{04}/Df(2R)\ BSC345$ (E), homozygous $vam^{c}$ (F), hemizygous $vam^{c}/Df(2R)\ BSC345$ (G) homozygous $Vam^{c};\ Vam{:}GFP$ (H) flies. Arrows point to the crossveins. (I) Histogram of relative wing areas in flies of the genotypes in panels C–H, as indicated. (J) Histogram of crossvein distances (CVD) (normalized to wing length) in flies of the genotypes in panels C–H, as indicated. (K–P) Adult male prothoracic legs from wild-type control (K), homozygous $vam^{04}$ (L), hemizygous $vam^{04}/Df(2R)\ BSC345$ (M), homozygous $vam^{c}$ (N), hemizygous $vam^{c}/Df(2R)\ BSC345$ and (O) homozygous $Vam^{c};\ Vam{:}GFP$ (P) flies, with the leg regions identified (tr, trochanter; fe, femur; ti, tibia; ta, tarsus). (Q) Histogram of relative tarsal lengths in flies of the genotypes in panels K–P. Data are shown

as mean ± SEM from measurements of 10–15 wings/legs per genotype. *$P$<0.001 (Student's $t$ test between wild-type control and the different genotypes); *NS*, not significant. See also Fig. S1.

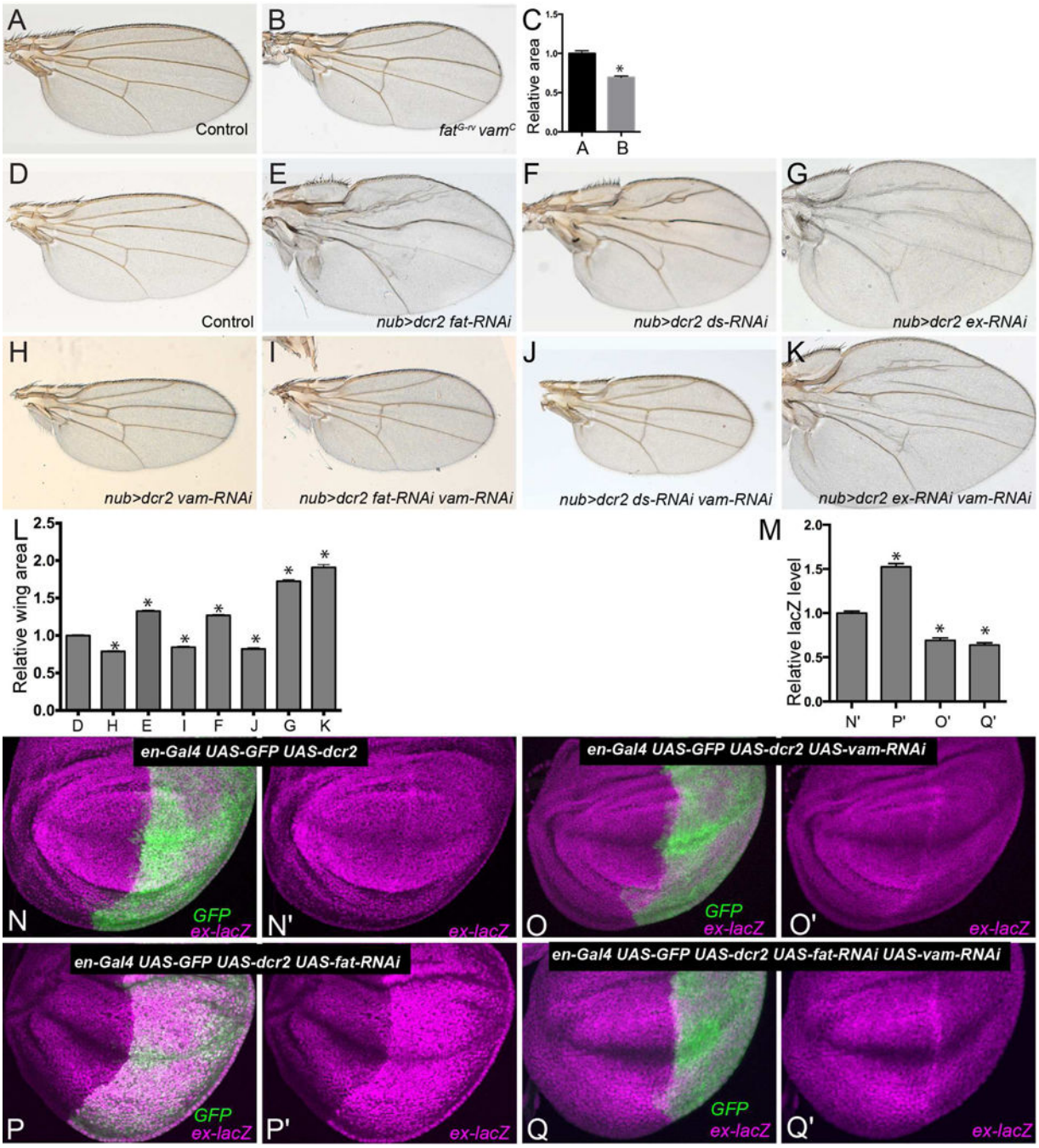


**Figure 2. *vam* is Epistatic to *fat***

Adult male wings from $w^{1118}$ control (A) and homozygous $ft^{G\text{-}rv}$ $vam^{c}$ mutant (B) flies. (C) Quantification of relative wing areas of the genotypes shown in A and B. Data are shown as mean ± SEM from measurements of 8–12 wings per genotype. *$P$ <0.001 (Student's $t$ test). D–K) Adult male wings from flies expressing *nub-Gal4 UAS-dcr2* (control)(D), *nub-Gal4 UAS-dcr2 UAS-fat-RNAi* (E), *nub-Gal4 UAS-dcr2 UAS-ds-RNAi* (F), *nub-Gal4 UAS-dcr2 UAS-ex-RNAi* (G), *nub-Gal4 UAS-dcr2 UAS-vam-RNAi* (H) *nub-Gal4 UAS-dcr2 UAS-fat-RNAi UAS-vam-RNAi* (I), *nub-Gal4 UAS-dcr2 UAS-ds-RNAi UAS-vam-RNAi* (J), *nub-*

*Gal4 UAS-dcr2 UAS-ex-RNAi UAS-vam-RNAi* (K). L) Histogram of relative wing areas in flies of the genotypes shown in panels D–K. M) Histogram of ratio of lacZ levels in the posterior compartments relative to the anterior compartments, in third instar wing imaginal discs from flies of the genotypes shown in panels N–Q, normalized to the mean ratio from control flies. (N–Q) Third instar wing imaginal discs expressing *en-Gal4 UAS-dcr2 UAS-GFP ex-lacZ* (N, N′) and *UAS-fat-RNAi* (P, P′) *UAS-vam-RNAi* (O,O′) *UAS-fat-RNAi* and *UAS-vam-RNAi* (Q, Q′), stained for expression of *ex-lacZ* (magenta), with posterior cells marked by expression of GFP (green). Data are shown as mean ± SEM from measurements of 10–12 wings/wing discs per genotype, error bars indicate SEM. **P*<0.001 (Student's *t* test between control and the other genotypes). See also Fig. S2.

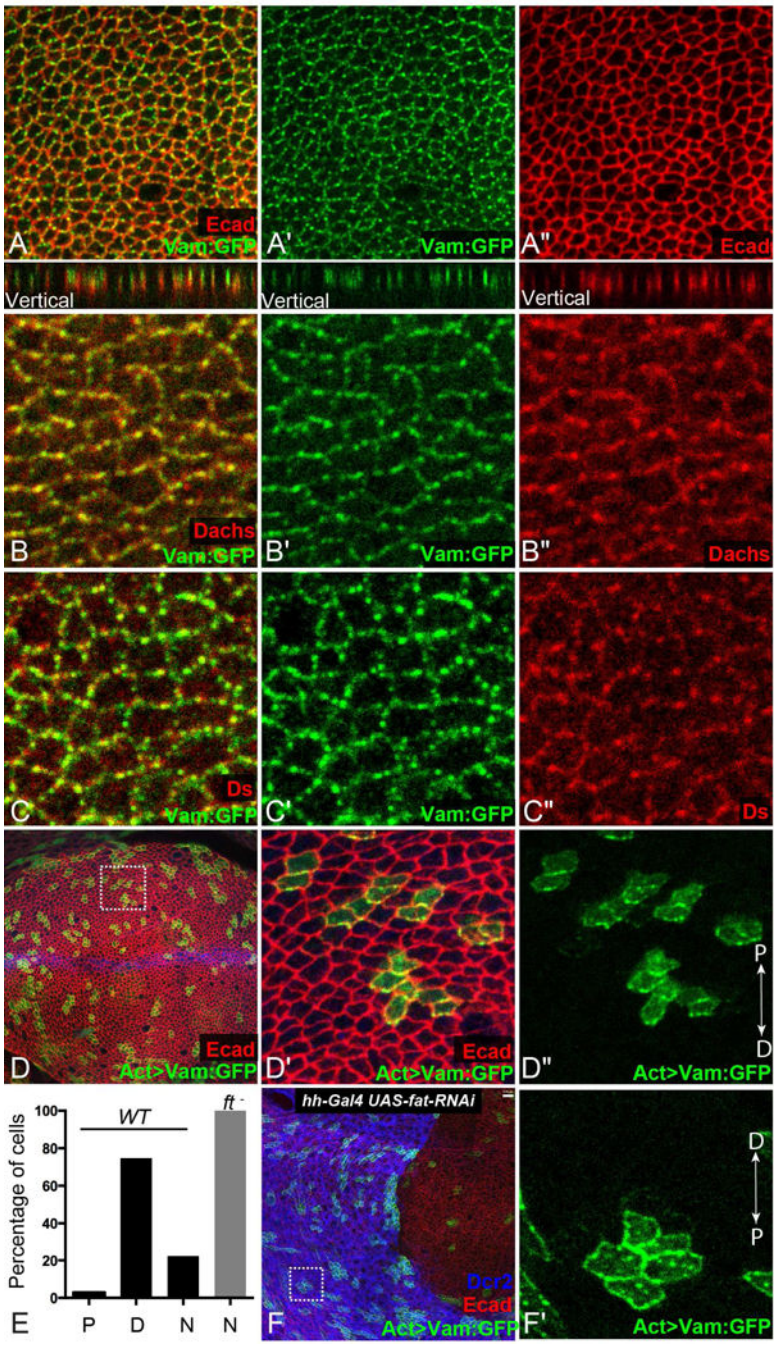


**Figure 3. Localization of Vam in Wing Imaginal Discs**

A–C) Localization of Vam in the wing discs of animals carrying a GFP-tagged genomic copy of vam (Vam:GFP)(green) relative to E-cad (red) (A,A′,A″), Dachs (red) (B, B′,B″) and Ds(C, C′, C″) in apical horizontal sections; a vertical section is also shown for A. D) Wing disc showing Vam:GFP localization in flip-out clones, expressed from an Actin5C promoter, in an apical horizontal section relative to Ecad (red) and the dorsal ventral compartment boundary marked by Wg staining (blue). Close up view of Vam:GFP localization in the boxed area is at right (D′, D″) showing Vam:GFP enriched on distal cell

junctions. The arrows indicate the proximal (P)-distal (D) orientation. E) Histogram showing percentage of cells showing proximal (P), distal (D) or neither (N) polarization of Vam-GFP in wild-type (WT) (total scored = 690) or fat depleted (*ft*) cells (total scored = 320); in wild-type discs, cells without clear distal polarization are preferentially found near the D–V boundary. F) Vam:GFP in flip-out clones in Wing disc expressing fat-RNAi in the posterior compartment under hh-Gal4 control, marked by Dcr2 staining (blue). A close up of the boxed area showing accumulation of Vam:GFP around the entire perimeter of the clone is at right (F′). See also Fig. S3.

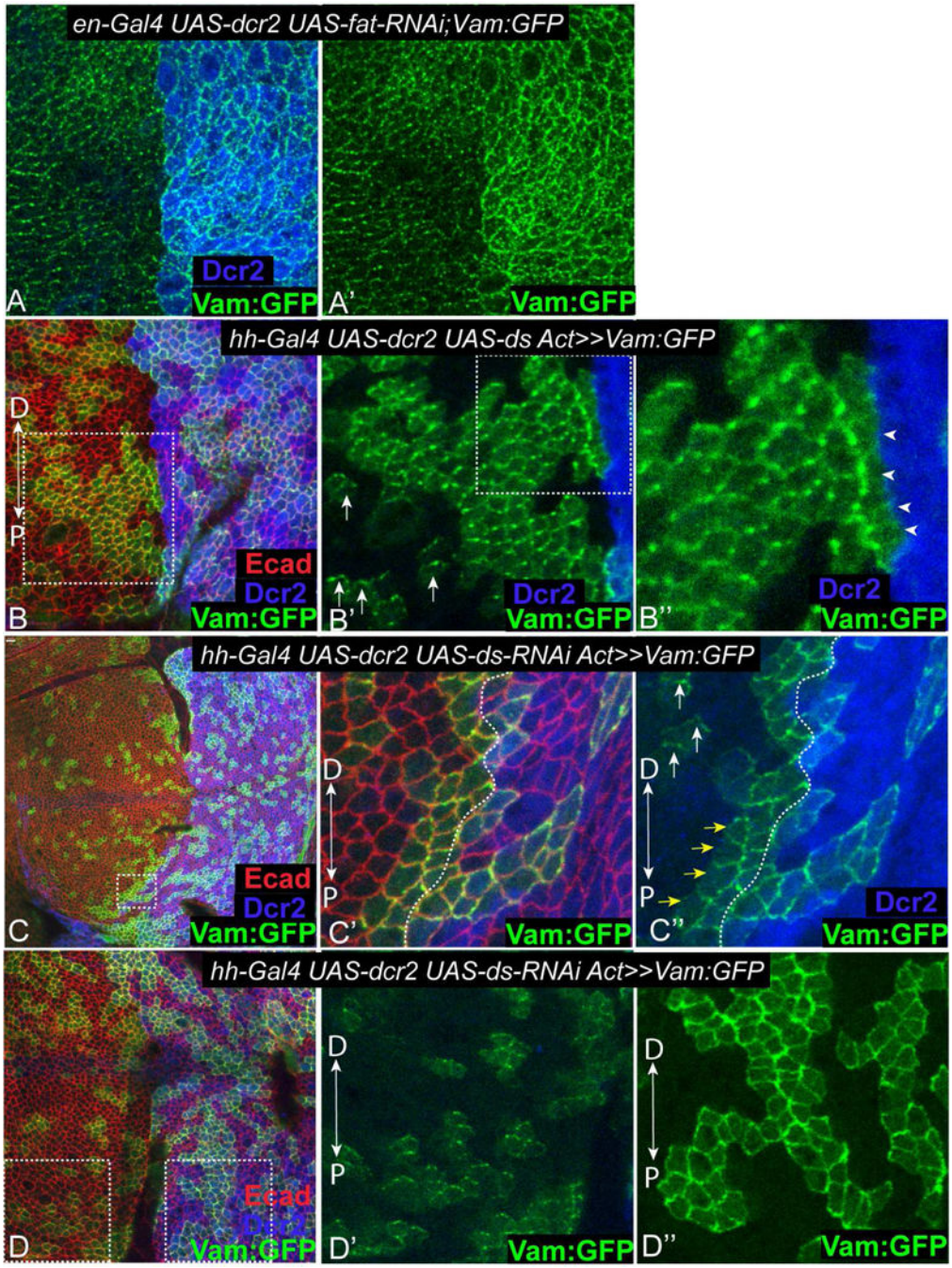


**Figure 4. Effect of Fat Signaling on Vam Localization**

A) Horizontal apical sections of wing discs expressing genomic Vam:GFP and A) en-Gal4 UAS-dcr2 UAS-fat-RNAi showing increase apical Vam:GFP upon depletion of fat in posterior cells (marked by Dcr2 staining, blue). B–D) Horizontal apical sections of wing discs expressing Flip-out Vam:GFP hh-Gal4 UAS-dcr2 and either UAS-ds (B) or UAS-RNAi-ds (C,D), with posterior cells marked by Dcr2 (blue) and cell junctions marked by E-cad (red). In (B) higher magnification views of the boxed region are shown at right, arrows pointing to normal distal polarization of Vam:GFP (green), and arrow heads pointing to the

repolarization of Vam-GFP away from cells over-expressing Ds. In (C) white arrows point to normal distal polarization of Vam:GFP (green), and yellow arrows pointing to the repolarization of Vam-GFP towards cells depleted of Ds, and dashed line marks the edge of hh-driven expression. In (D) panels to right show Vam:GFP from boxed regions within anterior (wild-type localization) and posterior (Ds depleted) compartments; depletion of Ds leads to increased levels of Vam and loss of polarity.

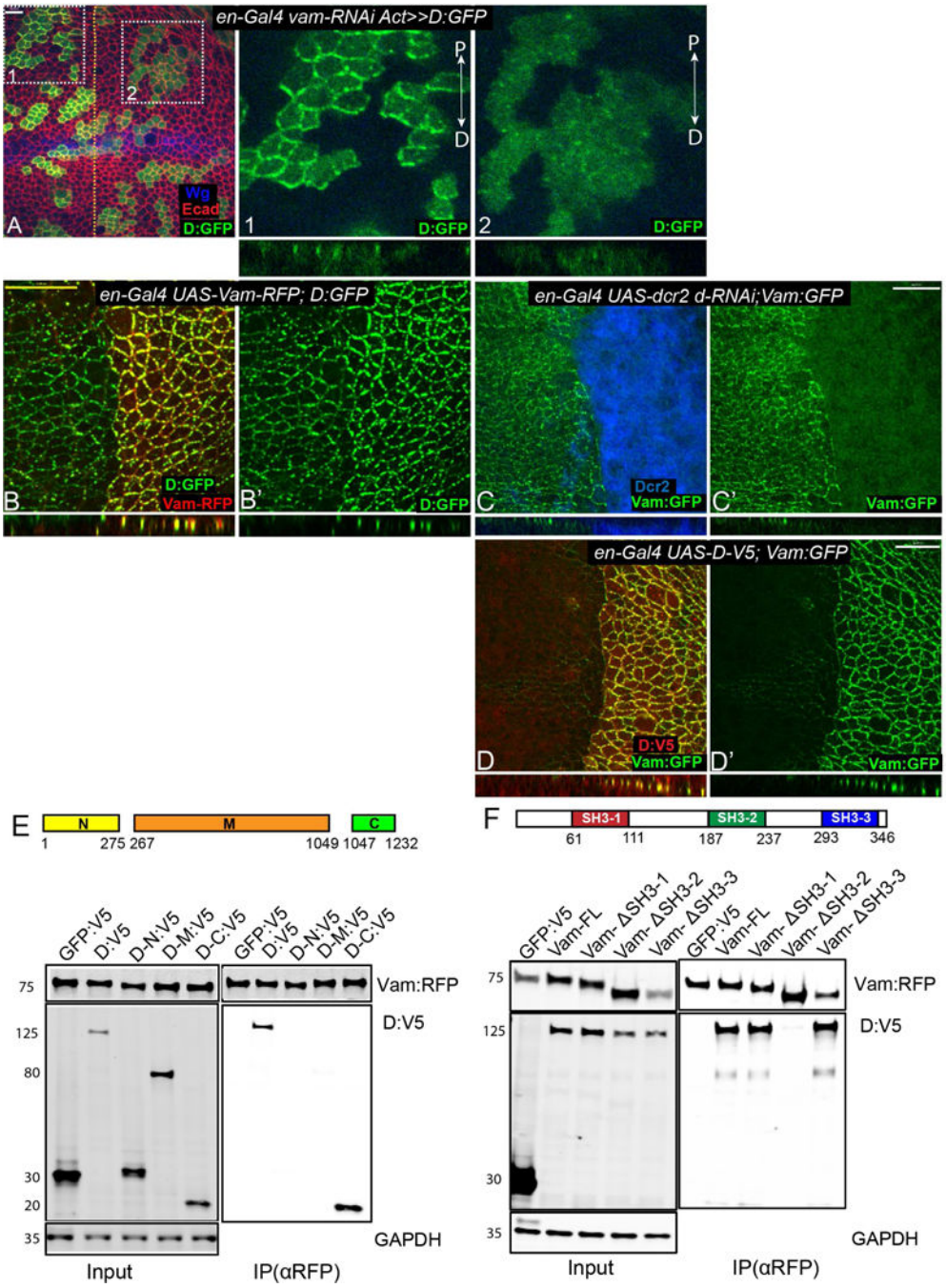


**Figure 5. Vam and Dachs Reciprocally Regulate each other and Physically Interact**

A) Wing imaginal disc expressing Dachs:GFP (*D:GFP*, green) in clones and *UAS-vam-RNAi* in posterior cells (right side) under *en-Gal4*, which leads to loss of junctional D:GFP. Right panels show close-ups of the anterior (1) and posterior (2) boxed areas. (B,B′) Horizontal (above) and vertical (below) sections of a wing disc expressing *en-Gal4 UAS-Vam:RFP (red); D:GFP* (green) showing increased junctional D:GFP in posterior cells. (C, C′) Horizontal (above) and vertical (below) sections of a wing disc expressing *en-Gal4 UAS-dcr2 UAS-d-RNAi; Vam:GFP* loss of membrane localization of Vam:GFP (green) in

posterior cells. (D,D′) Horizontal (above) and vertical (below) sections of a wing disc expressing *en-Gal4 UAS-D:V5 (red); Vam:GFP* (green) showing increased levels of membrane localized Vam:GFP in posterior cells. (E) Western blot showing results of co-immunoprecipitation experiments on proteins co-expressed in S2 cells. Schematic depicts the different Dachs fragments used with the amino acid numbers below. V5-tagged GFP (negative control), Full length Dachs (D:V5), D N terminus(D–N:V5), D Middle domain (D-M:V5) or D C terminus (D-C:V5) were co-expressed with full length Vam:RFP, and complexes were precipitated using RFP-trap. (F) Western blot showing results of co-immunoprecipitation experiments on proteins co-expressed in S2 cells. Schematic depicts Vam and the SH3 domain fragments used with the amino acid numbers below. V5-tagged GFP (negative control) or Full length Dachs (D:V5) were co-expressed with either full length Vam:RFP (Vam-FL) or Vam:RFP lacking the First (Vam-ΔSH3-1) second (Vam-ΔSH3-2) or third SH3 domain (Vam-ΔSH3-3), and complexes were precipitated using RFP-trap. GAPDH was used as a control for loading and transfer in the input lanes. See also Fig. S4.

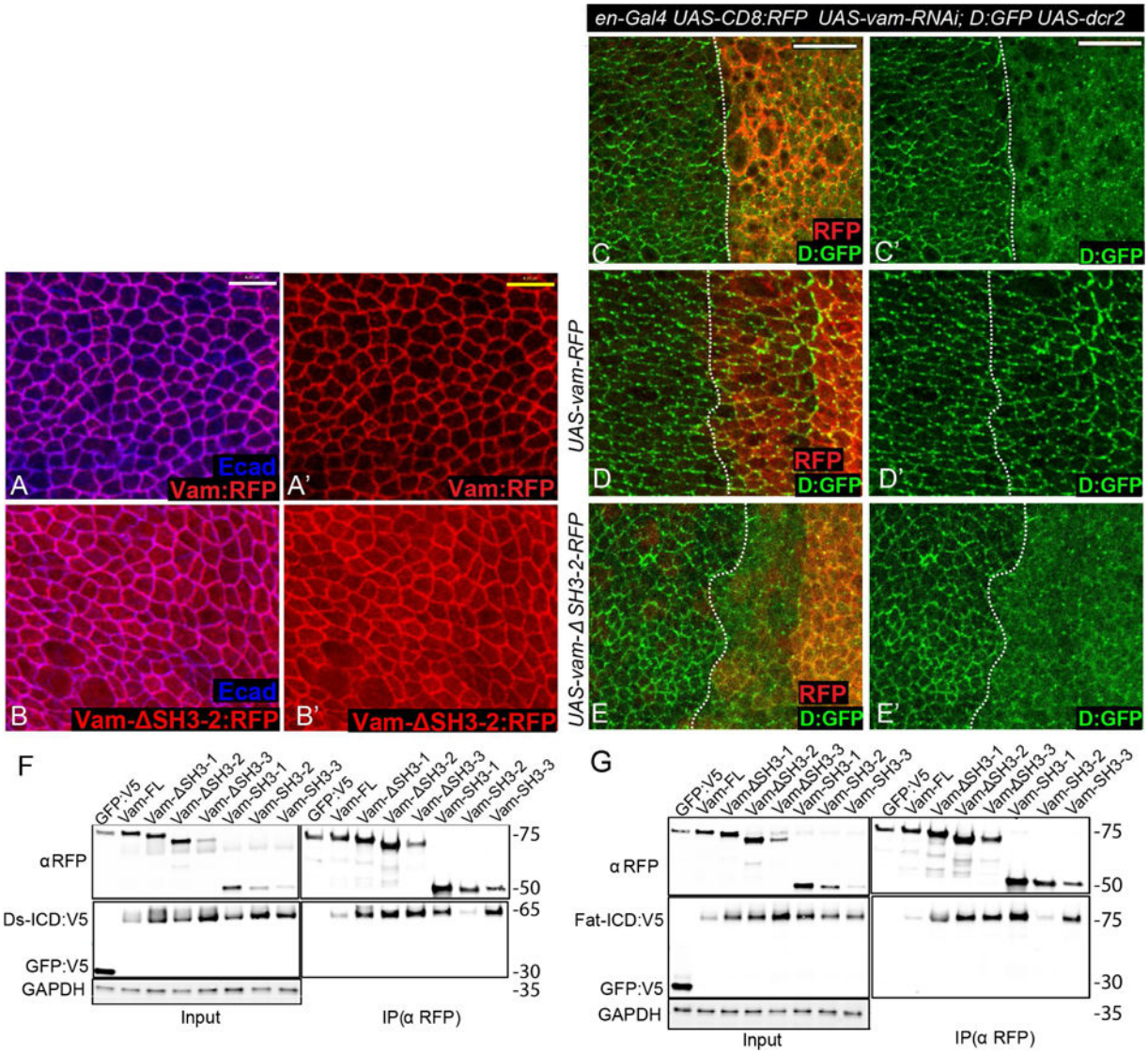


**Figure 6. Influence of Vam SH3 Domains on Dachs Localization**

A–B) Horizontal apical sections of wing imaginal discs expressing *nub-Gal4 and UAS-Vam-RFP* (A,A′) or *UAS-Vam-ΔSH3-2:RFP* (B,B′). C–E) Horizontal apical sections of wing imaginal discs expressing *Dachs:GFP* (D:GFP) *en-Gal4 UAS-CD8:RFP UAS-dcr2 UAS-Vam-RNAi* and also *UAS-Vam:RFP* (D,D′) or *UAS-Vam-ΔSH3-2* (E,E′). Depletion of endogenous Vam and simultaneous expression of Vam-RFP restores D:GFP membrane localization (D,D′), while expression of Vam-ΔSH3-2 (E,E′) fails to fully restore junctional D:GFP. Dashed white line marks approximate edge of en-Gal4 expression. F) Western blot showing results of co-immunoprecipitation by RFP-trap of V5-tagged GFP (negative control) or V5-tagged Ds-ICD (detected by anti-V5), co-expressed in S2 cells with either full length Vam:RFP (Vam-FL) or Vam-RFP lacking the first (Vam-ΔSH3-1) second (Vam-ΔSH3-2) or third SH3 domain (Vam-ΔSH3-1) or containing just the first (Vam-SH3-1) second (Vam-SH3-2) or third SH3 domain (Vam-SH3-3) G). Western blot showing results of co-immunoprecipitation by RFP-trap of V5-tagged GFP (negative control) or V5-tagged Fat-

ICD (detected by anti-V5), co-expressed in S2 cells with either full length Vam:RFP (Vam-FL) or Vam-RFP lacking the first (Vam-ΔSH3-1) second (Vam-ΔSH3-2) or third SH3 domain (Vam-ΔSH3-1) or containing just the first (Vam-SH3-1) second (Vam-SH3-2) or third SH3 domain (Vam-SH3-3)(G). See also Fig. S5.

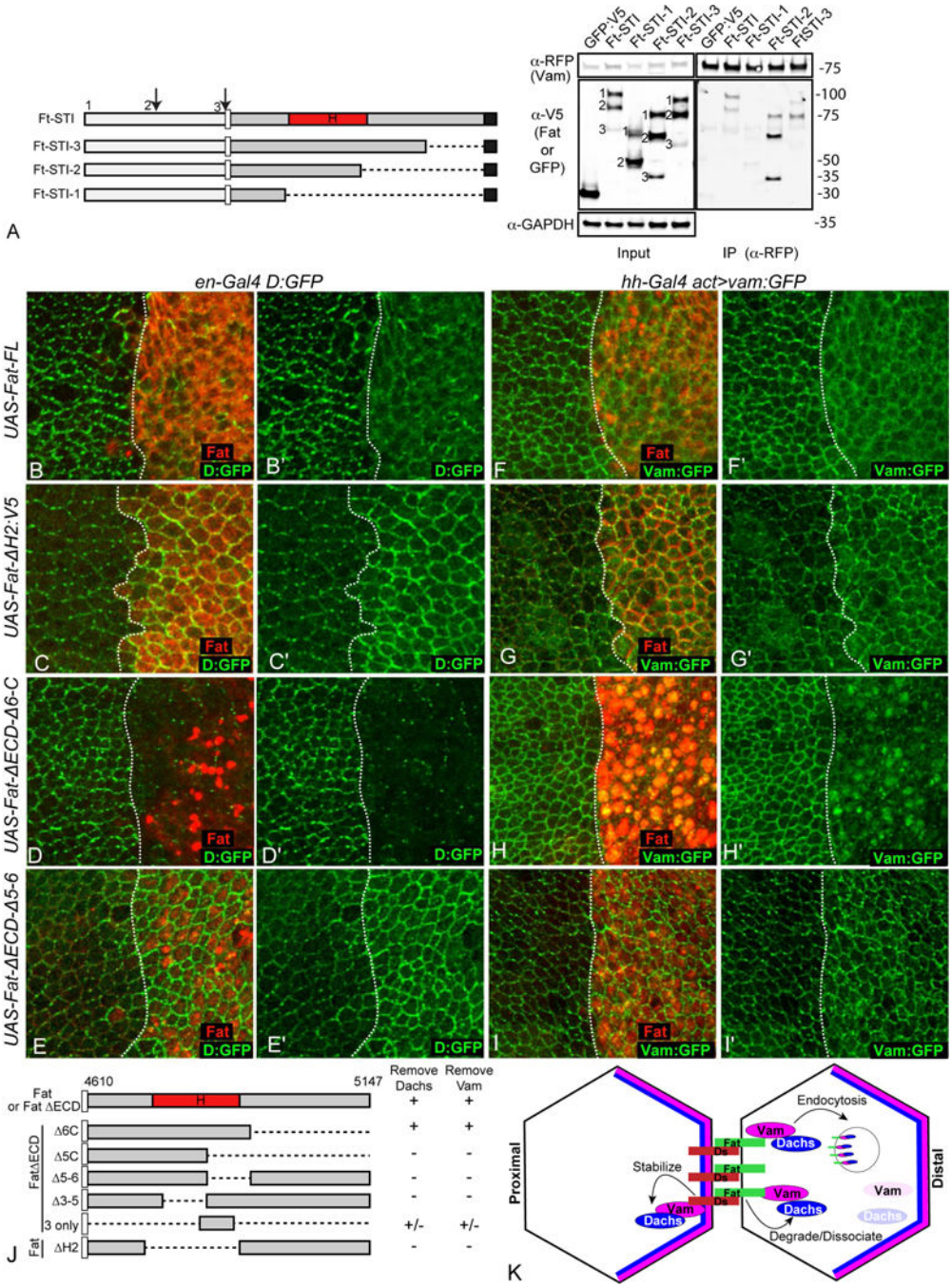


**Figure 7. Regulation Vam by the H Region of the Fat Intracellular Domain**

(A) Western blot showing results of co-immunoprecipitation using RFP-trap of V5-tagged GFP (negative control) or Full length Fat-STI or FAT-STI lacking different regions (detected by anti-V5), co-expressed in S2 cells with full length Vam-RFP (detected by anti RFP antibody). Schematic at left shows the different Fat constructs used for mapping the interaction between Vam and the Fat ICD, with the dashed lines indicating the amino acids absent. These Fat constructs (Feng and Irvine, 2009; Pan et al., 2013) are truncated at Fat amino acid 5023 (STI-3), 4885 (STI-2) and 4725 (STI-3). GAPDH was used as a control for

loading and transfer in the input lanes. Fat is subject to endoproteolytic cleavages (Feng and Irvine, 2009; Sopko et al., 2009), numbers indicate the bands corresponding to the full length proteins (1) and bands resulting from cleavage near the indicated locations. B–I) Horizontal apical sections of wing imaginal discs expressing either *en-Gal4; D:GFP (B–E) or hh-Gal4 act>> vam:GFP (F–I) and UAS-Fat-FL* (B,F), *UAS-Fat-ΔECD-ΔH2* (C,G), *UAS-Fat-ΔECD-Δ6-C* (D,H) and *UAS-Fat-ΔECD-Δ* 5-6 (E,I) showing their influence on apical membrane localization of D:GFP and vam:GFP when expressed in posterior cells (right side, marked by expression of tagged Fat (red) in panels without prime symbols). (J) Schematic showing the different Fat constructs assayed for their influence on Dachs and Vam here and in Fig S6 for their ability (+) or inability (−) to displace membrane localized D:GFP and Vam:GFP. K) Possible mechanisms for regulation of Dachs by Fat and Ds through Vam, see text for details. Depicted are Fat (green), Vam (purple), Dachs (blue) and Ds (red). See also Fig. S6 and S7.